International Journal of the Physical Sciences Vol. 6(3), 407-417, 4 February, 2011
Available online at http://www.academicjournals.org/IJPS
DOI: 10.5897/IJPS10.652
ISSN 1992 - 1950 ©2011 Academic Journals

*Full Length Research Paper*

# The effect of vents arrangement on the energy efficiency of a convenient store

**Yu-Lieh Wu**

Department of Refrigeration, Air-Conditioning and Energy Engineering, National Chin-Yi University of Technology, Taichung, Taiwan 411, R.O.C. E-mail: wuyl@ncut.edu.tw. Tel: 886-6-23924505 ext 8253; Fax: 886-6-23932758.

Accepted 13 January, 2011

**The objective of this paper is to investigate the energy efficiency of air conditioning via the viewpoint of the vents arrangement. In the research, a real typical convenience store located in Taichung, Taiwan is selected as a case study. The computational fluid dynamic (CFD) technique is adopted to simulate the flow, thermal and humidity distribution inside the convenient store under both close and open automatic door conditions. The results show that good air conditioning vents arrangement could lead the flow going through the path which could make sufficient heat exchange with the indoor air and increase the energy efficiency. The short-path should be avoided in order for the air that goes through one inlet vent to escape through another outlet vent directly such that the fresh air could not make mixture and heat exchange with the indoor air. The present methodology of integrating CFD simulation and experiments is powerful to make fast and accurate design on the design of air conditioning vents layout.**

**Key words:** Convenient stores, computation fluid dynamics, flow distribution, energy efficiency.

## INTRODUCTION

As a convenience store has refrigeration equipments to keep refrigerated foods and beverages, service equipments, a microwave, heating equipments for hot foods, air conditioning, indoor lighting and opens for twenty-four hours, so it becomes the highest power consuming density places among the retail chain stores. It is very important to design and plan the convenience stores to operate at a low power consuming condition, but still keep the environment with convenience, comfort and the quality of foods, such that it could achieve the objective of energy saving and carbon reduction.

In recent years, most literatures of the convenience stores are related to the enhancement of the refrigeration equipment performance. Particularly, there are many design improvements on the open display cabinets which include the computational fluid dynamics (CFD) technique and the full size experimental measurements verified to make the flow distribution analysis and the modification on the exhaust vents. For example, Gary et al. (2008) experimentally investigated the effect of the rear airflow opens of the vertical open display cabinet on the inner airflow distribution of the cabinet. The results found show that the proper opens are helpful to obtain the appropriate airflow and temperature distributions. Amin et al. (2008) and (Mazyar et al., 2008) adopted tracer gas technique to measure the heat drawn into the rate of the open display cabinet. Navaz et al. (2004, 2006) applied the digital particle image velocimetry (DPIV) to measure the velocity distribution and Reynolds number of the open display cabinets under different airflow velocity and angle through the air curtain. They also used FLUENT, a commercial CFD software, to make the simulation. The results were compared with the measurements. Chen et al. (2005) experimentally discussed the effect of the ambient temperature, indoor relative humidity, environmental airflow velocity, the airflow velocity from the air curtain and the airflow opens of the back plate on the temperature distribution and heat loads of the open display cabinet with single array air curtain. Hsieh et al. (2009) adopted CFD to discuss the effect of 3D end effects on velocity and temperature among layers of the vertical open display cabinet. They found that the secondary vortex which leads the heat drawn into such layers might affect the velocity of air curtain and the inner temperature distribution of the display cabinet.

In order to efficiently reduce the power consumption of the convenience stores, there is need not to develop only the high efficient and economic equipments, but also to decrease the power consumption of the air conditioning system. However, there is no standard that should be followed about the layouts of air outlets and return air inlets. Therefore, this paper applies the CFD simulation technique associated with the experimental to discuss the velocity, temperature and humidity distribution under different layouts of air outlets and return air inlets of a convenience store. The corresponding energy efficiency is also obtained and compared based on the simulation data. The effect of the layout of the air-conditioning outlets is also discussed based on the developed strategy.

## METHODOLOGY

### CFD simulation

The computer simulation technique has been widely applied to analyze the airflow phenomena. The beginning of the study of the indoor turbulent flow phenomena was conducted by the k-ε model developed by Launder and Spalding (1972, 1974) which was gradually referred and amended to make the characterization of the indoor turbulent flow more suitable in the study. For example, Nielsen et al. (1978) applied the k-ε model proposed by Pope and Whitelaw (1976) to study the characterization of the regional velocity and thereafter proposed the investigation of the indoor airflow with small vents. Kurabuchi and Kusuda (1987) also made in-depth discussion of the simulation prediction of the regional airflow distribution, while Awbi (1989) used the numerical method to establish the 2D and 3D steady-state model to predict the distribution of the flow and temperature fields of the ventilation space.

In this research, the 3D computation fluid dynamics base has been applied to make the simulation on a typical convenient store in Taiwan. The analysis of the flow and temperature fields is accomplished by numerically solving the continuity, moment and energy equations with standard k-ε turbulent model. The airflow behavior, considering the relative humidity, is simulated by adopting a two-phase mixture model. The CFD scheme used in this research is the finite volume method (FVM) and the computational domain is discredited into a finite set of control volumes. The general conservation (transport) equation for mass, momentum, energy, etc., are discredited into algebraic equations. The flow behavior of the air with relative humidity is treated as a two phase mixture flow.

The mixture model simulates the flow phenomena with two or more phases, treated as interpenetrating continua which allows the phases to be interpenetrated similarly to the mixing phenomena process. The volume fraction of each phase can be equal to any value between 0 and 1, depending on the space occupied by the phase. In the present studies, the phases are moved at different velocities using the slip velocities concept. The mixture model solves the continuity equation for the mixture, the momentum equation for the mixture, and the volume fraction equation for the secondary phases. The primary phase is the air and the secondary phase is the water vapor. Then the relative humidity of the airflow field can be converted by the volume fraction occupied by the water vapor.

The basic equations of the mixture model are shown as follows (Patanker, 1980; Fluent 6.3 User's Guide, 2007).

The continuity equation of the mixing fluid is:

$$\frac{\partial}{\partial t}(\rho_m) + \nabla.(\rho_m \vec{v}_m) = 0 \quad (1)$$

where $\vec{v}_m$ is the velocity of the mixing fluid,

$$\vec{v}_m = \frac{\sum_{k=1}^{n} \alpha_k \rho_k \vec{v}_k}{\rho_m} \quad (2)$$

where $\rho_m$ is the density of the mixing fluid, and

$$\rho_m = \sum_{k=1}^{n} \alpha_k \rho_k \quad (3)$$

where $\alpha_k$ is the volume occupation percentage of the kth phase.

The moment equation of the mixing fluid is:

$$\frac{\partial}{\partial t}(\rho_m \vec{v}_m) + \nabla \cdot (\rho_m \vec{v}_m \vec{v}_m) = -\nabla_p + \nabla \cdot [\mu_m (\nabla \vec{v}_m + \nabla \vec{v}_m^T)] + \rho_m \vec{g} + \vec{F} + \nabla \cdot \left(\sum_{k=1}^{n} \alpha_k \rho_k \vec{v}_{dr,k} \vec{v}_{dr,k}\right) \quad (4)$$

Where n is the nth phase, $\vec{F}$ is the body force and $\mu_m$ is the dynamic viscosity of the mixing fluid,

$$\mu_m = \sum_{k=1}^{n} \alpha_k \mu_k \quad (5)$$

$$\vec{v}_{dr,k} = \vec{v}_k - \vec{v}_m \quad (6)$$

Where $\vec{v}_{dr,k}$ is the drift velocity of the secondary phase.

The relative velocity is defined as the velocity of a secondary phase (p) relative to the velocity of the primary phase (q):

$$\vec{v}_{pq} = \vec{v}_p - \vec{v}_q \quad (7)$$

The mass fraction for any phase (k) is defined as:

$$c_k = \frac{\alpha_k \rho_k}{\rho_m} \quad (8)$$

The drift velocity and relative velocity could then be connected:

$$\vec{v}_{dr,p} = \vec{v}_{pq} - \sum_{k=1}^{n} c_k \vec{v}_{qk} \quad (9)$$

The volume fraction equation for secondary phase p can be obtained using the continuity equation for secondary phase p:

$$\frac{\partial}{\partial t}(\alpha_p \rho_p) + \nabla \cdot (\alpha_p \rho_p \vec{v}_m) = -\nabla \cdot (\alpha_p \rho_p \vec{v}_{dr,p}) + \sum_{q=1}^{n} (\dot{m}_{qp} - \dot{m}_{pq}) \quad (10)$$

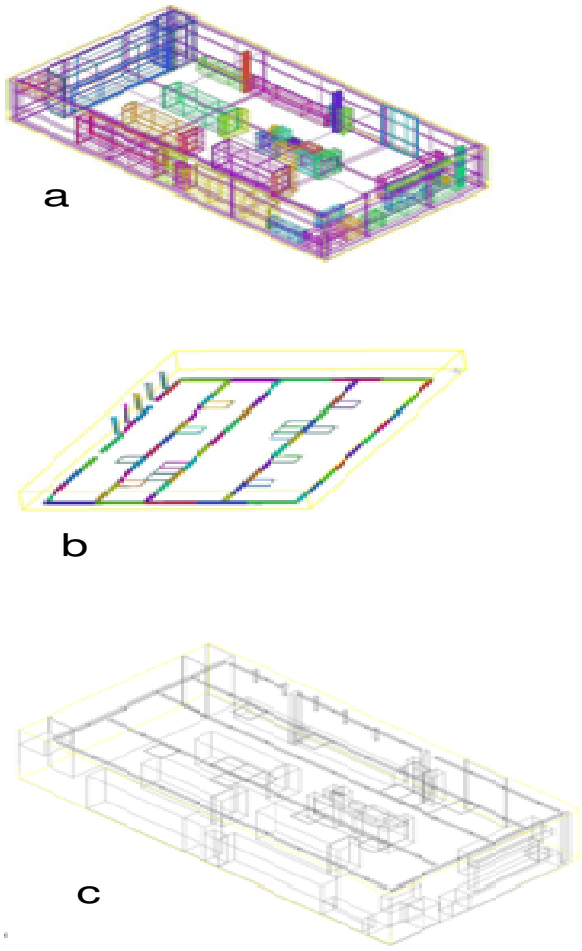


**Figure 1.** The geometry construction of the CFD model. (a) The indoor layout, (b) The ceiling, (c) The whole model of the convenient store.

The CFD simulation adopts 3D, steady-steady and zero-equation turbulence model. The gravity, radiation and humidity are considered.

### Experimental measurements

In order to confirm the reliability and accuracy of the CFD simulation, the research further made the actual field measurements on the selected points of the velocity, temperature and humidity values inside the convenient store and the data were compared with the simulation results.

### CFD model construction

The geometry of the CFD model was constructed based on the real layout and dimensions of the present convenient store. Figure 1 is the CFD model of the convenient store including the indoor layout, the ceiling and the whole model.

After the geometry construction, the mesh construction was conducted by the hexagonal unstructured mesh. The number of nodes of the convenient store was about 930,000 and the number of nodes that extended the outdoor ambient was about 1,730,000.

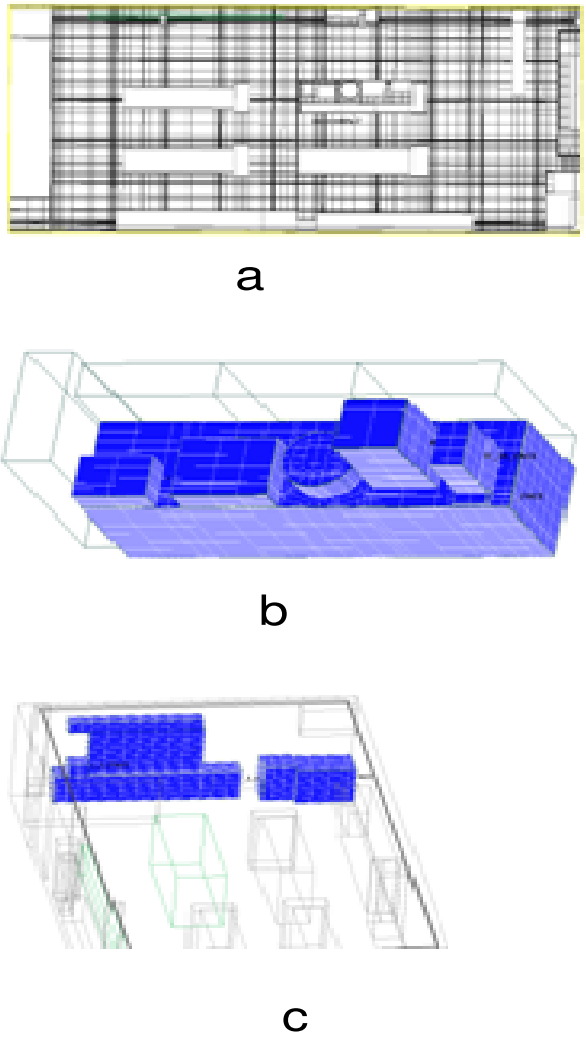


**Figure 2.** The mesh of CFD model of the convenience store. (a) A plane cut view inside the store, (b) The hot food area, (c) The objects behind the counter.

Figure 2 shows the mesh of the CFD model of the convenience store. Figure 2(a) is a plane cut view inside the store, while Figure 2(b) is the hot food area, and Figure 2(c) is the objects behind the counter.

### The setting of supply air and return air vents

The setting of the CFD model was based on the real measurement data on temperature, relative humidity and airflow velocity. Table 1 was the concluded measurement data under the close door condition and Table 2 was the concluded measurement data under the open door condition. All of the supply air vent's size is 60 × 60 cm and every air flow rate is shown in Table 3.

### The setting of the outdoor ambient and indoor heat sources

The related setting of the outdoor ambient and indoor heat sources is shown in Tables 4 and 5.

**Table 1.** Concluded measurement data of the supply and return air vents under the close door condition.

| | |
|---|---|
| Average dry bulb temperature of the supply air vents (□) | 15.9 |
| Average relative humidity of the supply air vents (%) | 89% |
| Average mass flow rate of the supply air vents (kg/s) | 0.15 |
| Average dry bulb temperature of the return air vents (□) | 22.6 |
| Average relative humidity of the return air vents (%) | 63 |
| Average mass flow rate of the return air vents (kg/s) | 0.14 |

**Table 2.** Concluded measurement data of the supply and return air vents under the open door condition.

| | |
|---|---|
| Average dry bulb temperature of the supply air vents (□) | 16.2 |
| Average relative humidity of the supply air vents (%) | 88 |
| Average mass flow rate of the supply air vents (kg/s) | 0.15 |
| Average dry bulb temperature of the return air vents (□) | 22 |
| Average relative humidity of the return air vents (%) | 63.1 |
| Average mass flow rate of the return air vents (kg/s) | 0.14 |

**Table 3.** All measurement data of the supply air flow rate of eight supply air vents.

| | | | | |
|---|---|---|---|---|
| No. of the supply air vent | 1 | 2 | 3 | 4 |
| Air flow rate ($m^3$/hr) | 568 | 495 | 387 | 327 |
| No. of the supply air vent | 5 | 6 | 7 | 8 |
| Air flow rate ($m^3$/hr) | 373 | 494 | 470 | 502 |

**Table 4.** Outdoor ambient.

| | |
|---|---|
| Outdoor ambient | |
| Outdoor ambient dry bulb temperature ($^oC$) | 33.4 |
| Outdoor ambient relative humidity (%) | 56 |
| Pressure difference between outdoor and indoor (Pa) | -1.5 |

**Table 5.** Indoor heat sources.

| **Lamps** | |
|---|---|
| Long fluorescent tube×53 (W) | 32×53 |
| Short fluorescent tube×7 (W) | 18×7 |
| Pendant lamp×5(W) | 26×5 |
| **Hot food equipments** | |
| The Guandong boils machine (W) | 1500 |
| Hot dog machine (W) | 936 |
| Electric rice cooker (W) | 800 |
| Steamed stuffed buns machine (W) | 950 |
| Total indoor heat load (W) | 6138 |

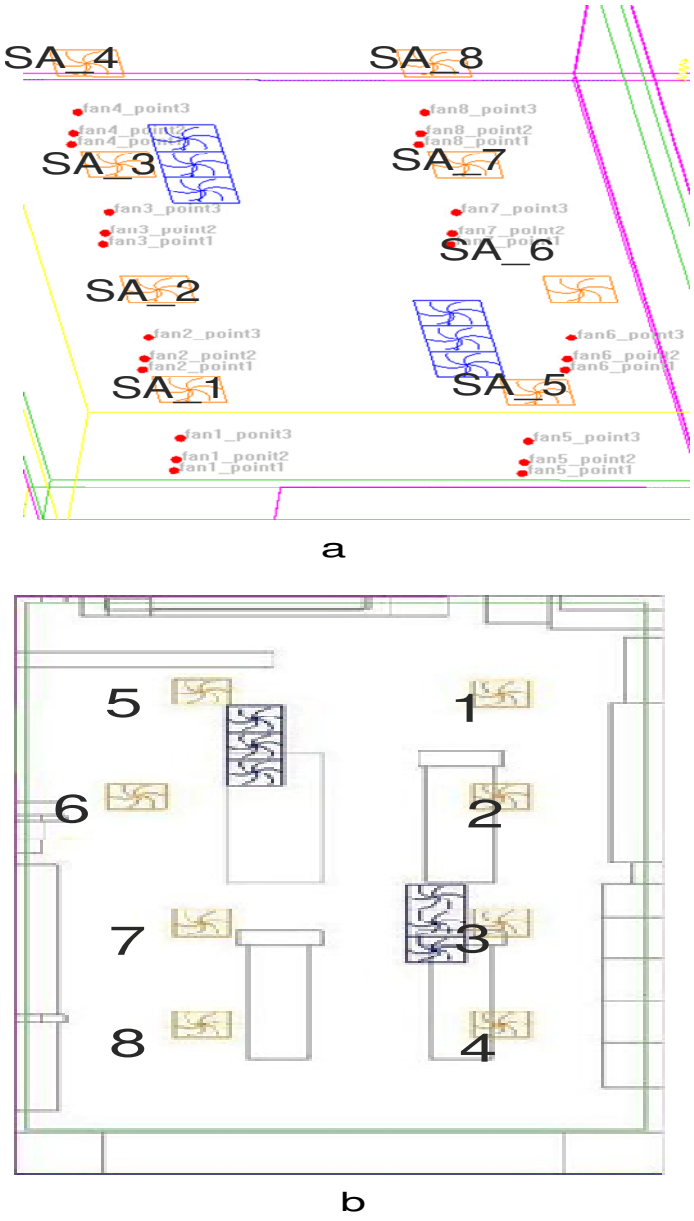


**Figure 3.** Illustration of the monitored points behind the supply air vents.

## Comparison of the simulation and experimental results

### *Closed door condition*

In order to verify the accuracy of the CFD simulation, the comparison of the simulation and experimental results of the closed door condition was first conducted. Figure 3 is the illustration of the monitored points behind the supply air vents. “SA” means air supply vent. Figures 4 and 5 are the plots of temperature and humidity for different air supply vents at 130 and 150 cm height under closed door condition, respectively.

### *Open door condition*

In the real operation, the automatic door of the convenient store will be open and closed along with the customers entering or going out. In order to investigate the effect of the layout of the air conditioning vents on energy consumption, the simulation for the open door condition will be discussed. The changes of the flow, temperature and humidity fields are then evaluated after the mixture of the outdoor and indoor air. Figures 6 and 7 are the plots of temperature and humidity for different air supply vents at 130 and 150 cm height under the open door condition, respectively.

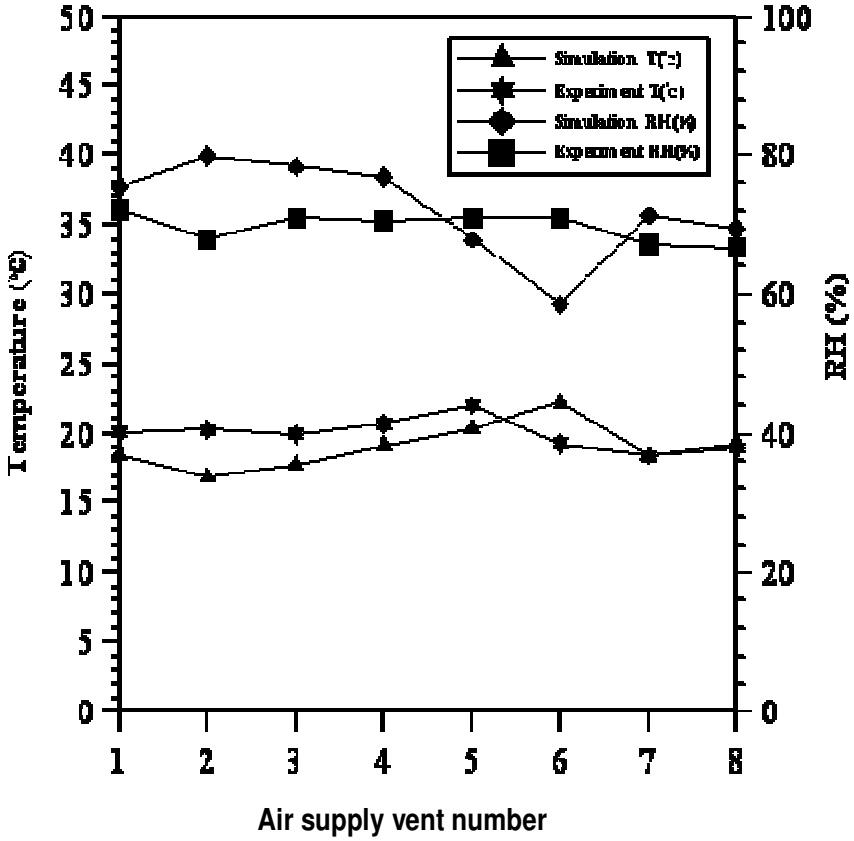


**Figure 4.** Plot of the temperature and humidity for different air supply vents at 130 cm height under the closed door condition.

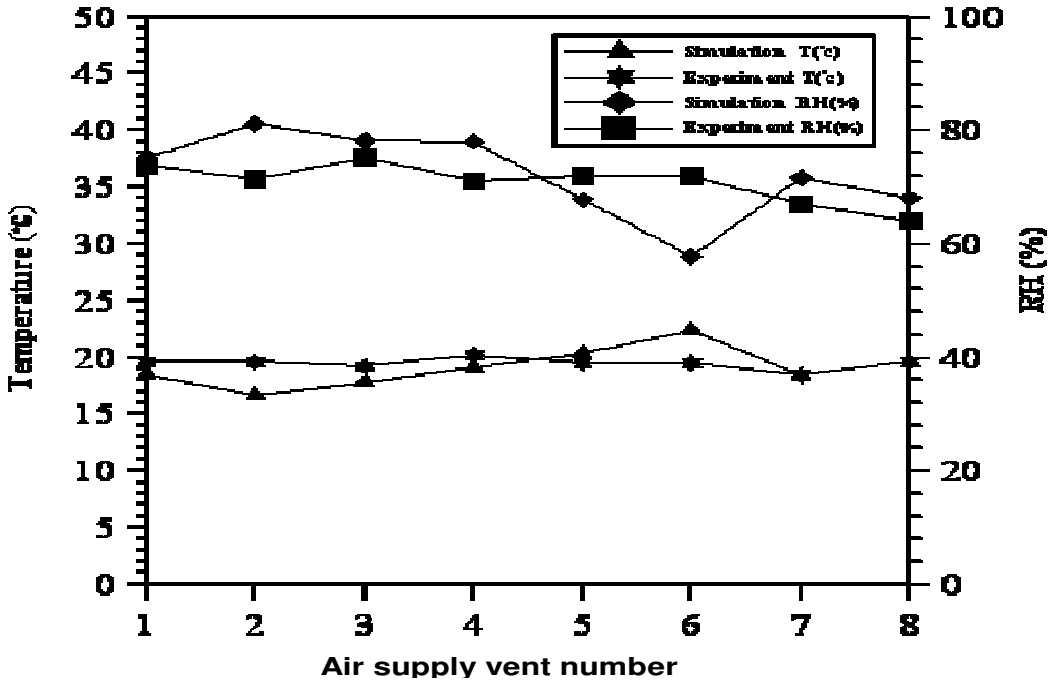


**Figure 5.** Plot of the temperature and humidity for different air supply vents at 150 cm height under the closed door condition.

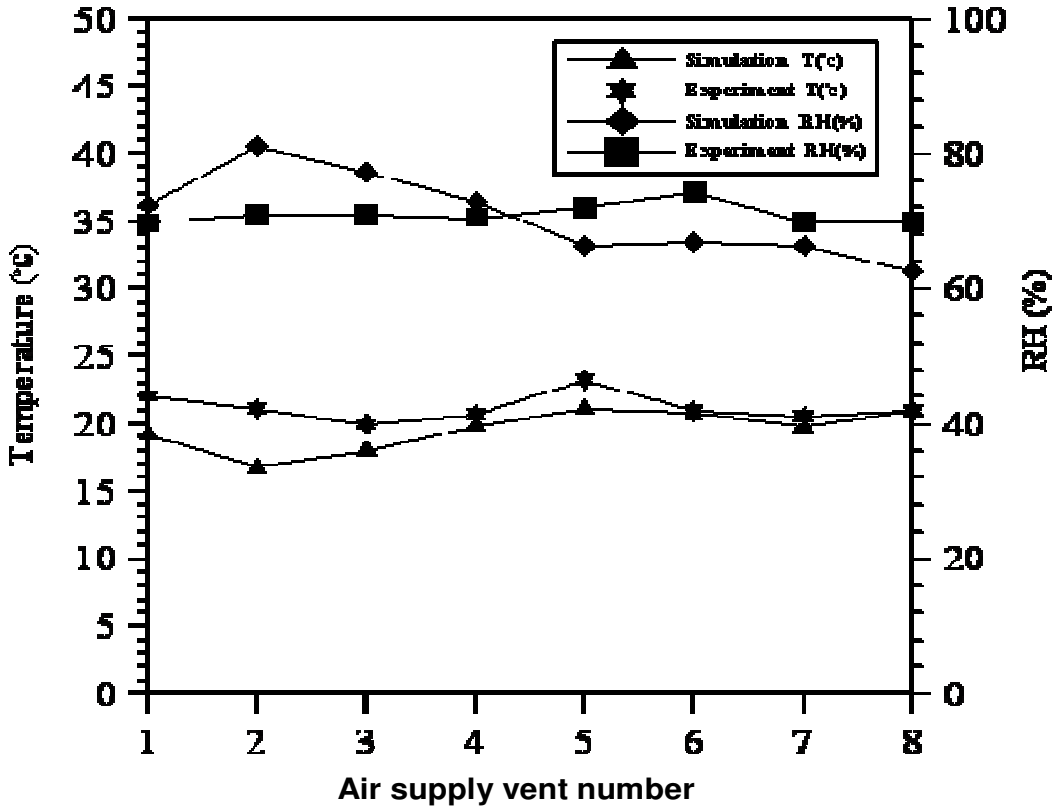


**Figure 6.** Plot of the temperature and humidity for different air supply vents at 130 cm height under the open door condition.

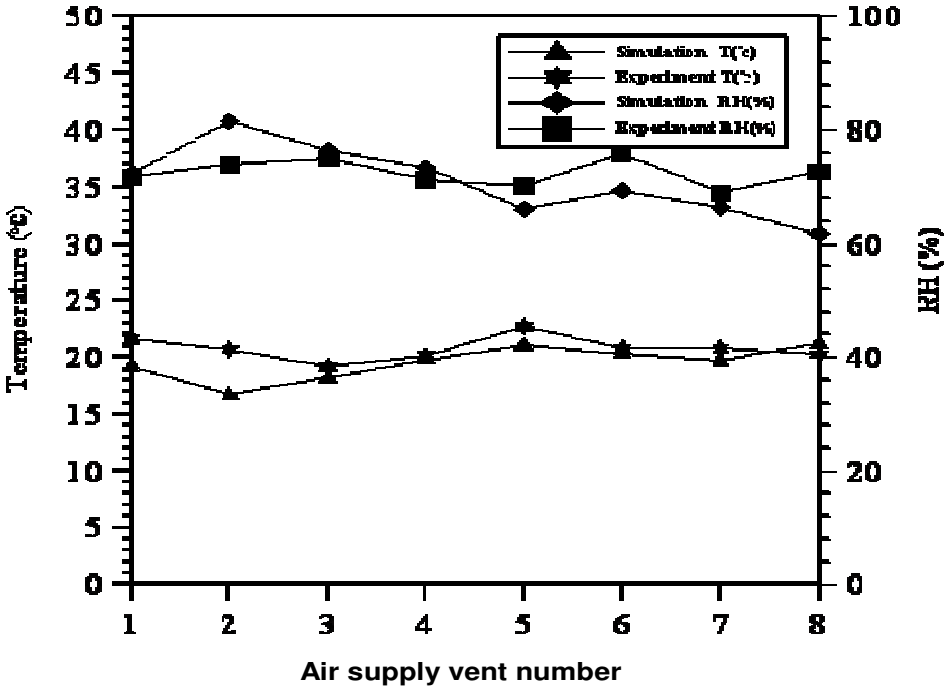


**Figure 7.** Plot of the temperature and humidity for different air supply vents at 150 cm height under the open door condition.

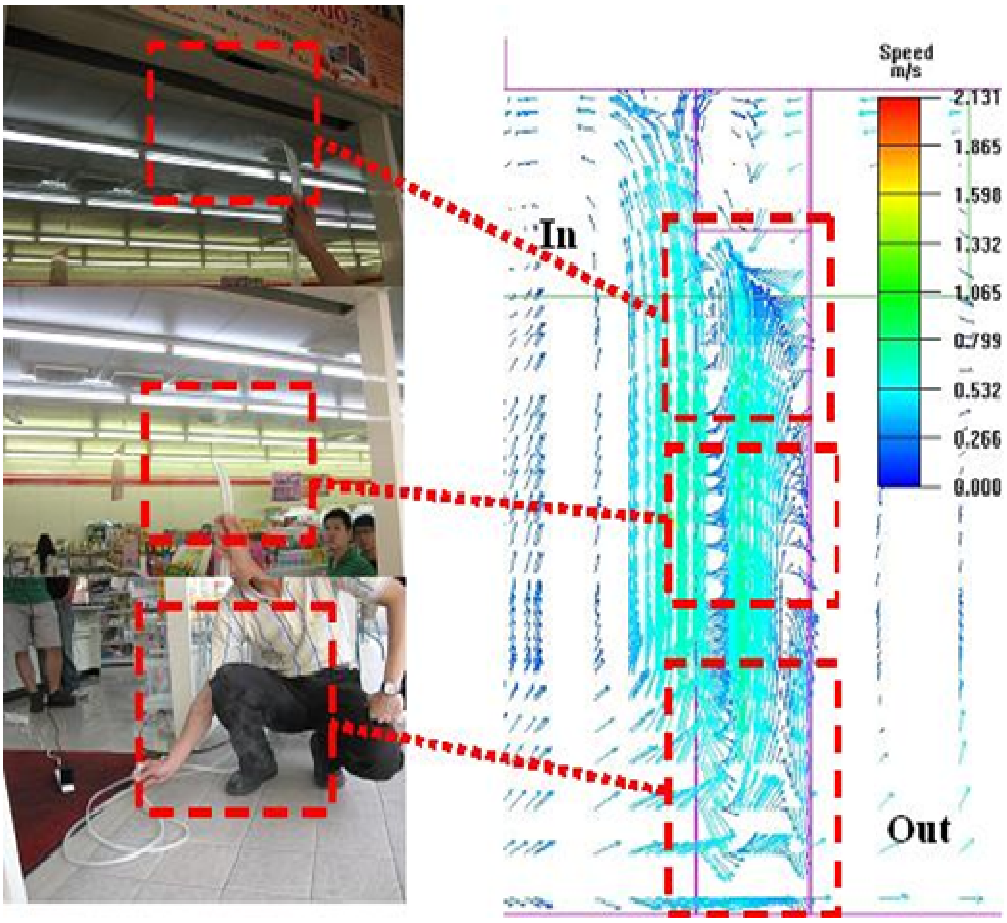


**Figure 8.** Comparison of the air flow smoke image and the CFD results at the open automatic door.

### Comparison of the airflow field at the automatic door

Figure 8 is the comparison of the air flow smoke image and CFD results at the open automatic door. The phenomena of the simulation results are conformed to the experimental images: that is, there is heat drawn into it from the upper place of the door and cold air loss through the bottom place of the door.

### Short circulation

In the present convenient store, there are six return air vents, but they are divided as two sets and each set contains three return air vents. In addition, the locations of the return air vents are quite close to the supply air vents. Particularly, the distance between the return air vent No.5 and the supply air vent No.3 is very short which leads the short circulation between these two vents. Both the CFD simulation and air smoke image could find the phenomena, as shown in Figure 9. Therefore, the layout of the air vents should be able to make some modification.

### Air vents layout versus energy saving

In order to investigate the relationship of the layouts of air vents and energy saving, the CFD model was further applied to make flow, temperature and humidity distribution at different layout of the air vents. Furthermore, the energy efficiency was evaluated based on the heat load model described as follows to analyze the effect of the layout of air vents.

### Calculation of heat removal rate

In the present study, the key issue of the calculation is the exclusion of the air-conditioning load. The standard of comparison is the indoor average temperature and the amount of air-conditioning load under different layout of air vents at closed or open door conditions. The formula of the heat removal rate is shown in Equation (1).

$$Q_T = \dot{m} \quad (h_o - h_i) \qquad (1)$$

Where

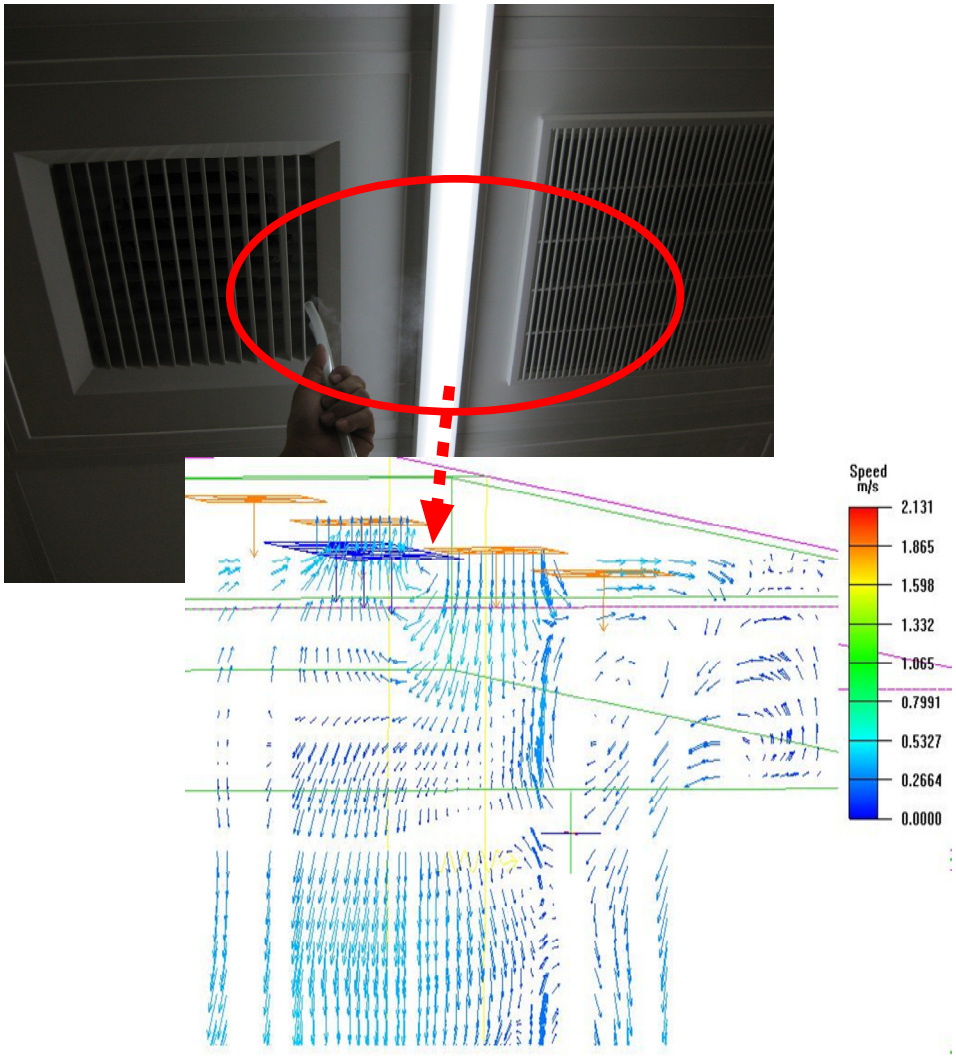


**Figure 9.** Short circulation phenomena.

**Table 6.** Average values of the related data and the exclusion heat load for the original air vent layout under the open door condition.

| | Temperature (℃ DB) | RH (%) | Enthalpy (kJ/kg d.a.) |
|---|---|---|---|
| Air supply vents | 16.3 | 87 | 41.48 |
| Return air vents | 22 | 63.13 | 48.61 |
| Outdoor | 23.3 | 63.19 | 52.18 |
| Indoor | 33.4 | 56 | 80.26 |
| Average airflow rate of the air supply vents | | 0.15 kg/s | |
| Exclusion heat load by air-conditioning | | 1.07kW | |

$Q_T$: Total heat load

$\dot{m}$ : Mass flow rate

$h_i$: Enthalpy of the air supply vent

$h_o$: Enthalpy of the return air vent

The average values from the CFD simulation of temperature, humidity, airflow rate for the original layout of air vents under the closed door condition are tabulated in Table 6. The enthalpy can be obtained based on these data. Then the total removal of the heat load by the

**Table 7.** Average values of the related data and the exclusion heat load for the original air vent layout under the closed door condition.

| | Temperature (℃ DB) | RH (%) | Enthalpy (kJ/kg d.a.) |
|---|---|---|---|
| Ambient | 33.4 | 56 | 80.26 |
| Indoor | 22.7 | 60.7 | 49.41 |
| Air supply vents | 16.3 | 87 | 41.85 |
| Return air vents | 21.6 | 64.14 | 47.97 |
| Average airflow rate of the air supply vents | | 0.14 kg/s | |
| Exclusion heat load by air-conditioning | | 0.86kW | |

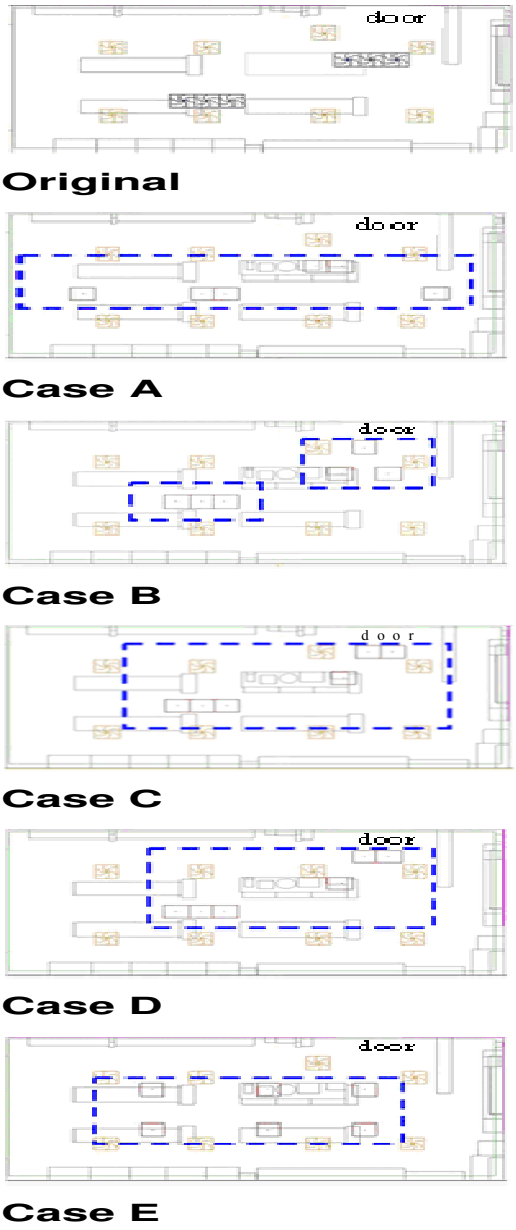


**Figure 10.** The layout of air vents for different cases.

air-conditioning can be calculated as 0.86 kW. The average values from the CFD simulation of temperature, humidity, airflow rate for the original layout of air vents under the open door condition are tabulated in Table 7. The enthalpy can be obtained based on these data. Then the total removal of the heat load by the air-conditioning can be calculated as 1.07 kW.

## Design change of the air vent layout

Five cases of the design change of the air vent layout were investigated here and were named Cases A to E. The different layouts of air vents for the original and design changes are shown in Figure 10. The airflow distribution with the information of temperature and humidity can be obtained by the CFD simulation. Then the exclusion heat load can be calculated based on Equation (1). The related data and results are tabulated in Table 8 and it could be found that Case D could get the better energy usage efficiency.

## Conclusions

This research successfully adopted CFD technique to simulate the airflow distribution of a typical convenient store. Based on the simulation results, the exclusion heat load by air-conditioning can be further estimated. The accuracy of the CFD model was first verified by the comparison with the experimental results. The results also show that improper layout of the airflow vents might lead to short circulation from the air supply vents to the return air vents. Five design changes on the layout of air vents were also performed in this research. If the placements of the return vents are adjusted only, Case E makes most of the improvement. It tells that the average distribution in the indoor space of the return air vents could provide better capability of the exclusion heat load and also reduce more average indoor room temperature. Overall, Case D shows the most improvement because the supply air vents blow towards the hot food area and as such, drives the high temperature air toward the door and will not stay inside the store.

**Table 8.** Comparison of the design change on the layout of air vents.

| | Original | Case A | Case B | Case C | Case D | Case E |
|---|---|---|---|---|---|---|
| Supply air vent temperature(℃ DB) | 16.2 | 16.3 | 16.2 | 16.2 | 16.2 | 16.5 |
| Supply air vent RH (%) | 88 | 87 | 88.01 | 88.05 | 88.02 | 87.3 |
| Supply Air vent enthalpy (kJ/kg d.a.) | 41.88 | 41.85 | 41.88 | 41.9 | 41.89 | 42.48 |
| Temperature of the return vent (℃ DB) | 22 | 22.1 | 21.8 | 22.1 | 21.4 | 22.1 |
| RH of the return air vents (%) | 63.13 | 62.37 | 62.5 | 61.97 | 64.37 | 62 |
| Enthalpy of the return vent (kJ/kg d.a.) | 48.61 | 48.55 | 47.81 | 48.38 | 47.53 | 48.39 |
| Indoor average temperature (℃ db) | 23.3 | 23.1 | 23.3 | 22.7 | 22 | 22.3 |
| Indoor average rh (%) | 63.2 | 63.1 | 63 | 62.4 | 64 | 63.1 |
| Indoor enthalpy (kJ/kg d.a.) | 52.18 | 51.59 | 52.1 | 50.17 | 48.98 | 49.4 |
| Outdoor temperature (℃ DB) | 33.4 | | | | | |
| Outdoor RH (%) | 56 | | | | | |
| Outdoor enthalpy (kJ/kg d.a.) | 80.26 | | | | | |
| Average mass flow rate of the air supply vents | 0.15 kg/s | | | | | |
| Exclusion heat load by air-conditioning (kW) | 1.07 | 1 | 0.89 | 0.97 | 0.85 | 0.89 |

## ACKNOWLEDGEMENT

The author sincerely acknowledges the financial support given by the Industrial Technology Research Institute of Taiwan throughout the research.

### REFERENCES

Awbi HB (1989). Application of computational fluid dynamics in room ventilation, Build. Environ., 24(1): 73-84.

Chen YG, Yuan XL, (2005). Experimental study of the performance of single-band air curtains for a multi-deck refrigerated display cabinet, J. Food Eng., 69: 261-267.

Fluent 6.3 User's Guide (2007). Fluent Inc.

Gray I, Luscombe P, McLean L, Sarathy GSP, Sheahen P, Srinivasan K (2008), Improvement of air distribution in refrigerated vertical open front remote supermarket display cases, Int. J. Refrig., 31: 902-910.

Hsieh WD, Chen YF, Dai CH (2009). Three-dimensional CFD simulation of multi-deck open retail display case. Refrigeration, Air-condition., Heat Trans., 88: 1-10.

Kurabuchi T, Kusuda T (1987). Numerical prediction for indoor air movement, ASHRAE J., December., 26-30.

Launder BE, Spalding DB (1972). Mathematical models of turbulence, Academic Press, London and New York.

Launder BE, Spalding DB (1974). The numerical computation of turbulent flows, Comput. Method. Appl. Mech. Eng., 3: 269-289.

Mazyar A, Dana D, Homayun KN. (2008), Tracer gas technique, A new approach for steady state infiltration rate measurement of open refrigerated display cases. J. Food Eng., (in press).

Navaz HK, Amin M, Rasipuram SC, Faramarzi R (2006). Jet entrainment minimization in an air curtain of open refrigerared display cases, Int. J. Numer. Method Heat Fluid Flow, 16(4): 417-430.

Navaz HK, Henderson BS, Faramarzi R, Pourmovahed A, Taugwalder F (2004). Jet entraiment rate in air curtain of open refrigerared display cases, Int. J. Refrig., 28: 267-275.

Nielsen PV, Restivo A, Whitelaw JH (1978). The velocity characteristic of ventilated rooms. J. Fluids Eng., 100: 291-298.

Patanker SV (1980). Numerical Heat Transfer and Fluid Flow, Hemisphere Publishing Co.

Pope SB, Whitelaw JH (1976). The calculation of near-wake flows, J. Fluid Mech., 73(1): 9-32.